LASER INTERFEROMETER GRAVITATIONAL WAVE OBSERVATORY
- LIGO -
CALIFORNIA INSTITUTE OF TECHNOLOGY
MASSACHUSETTS INSTITUTE OF TECHNOLOGY

Technical Note	**LIGO-T1300555-v1-**	2013/07/29

LIGO SURF Progress Report 1

Gautam Venugopalan
Mentors: Manasadevi P Thirugnanasambandam, Jenne Driggers, Rana Adhikari

California Institute of Technology
LIGO Project, MS 18-34
Pasadena, CA 91125
Phone (626) 395-2129
Fax (626) 304-9834
E-mail: info@ligo.caltech.edu

Massachusetts Institute of Technology
LIGO Project, Room NW22-295
Cambridge, MA 02139
Phone (617) 253-4824
Fax (617) 253-7014
E-mail: info@ligo.mit.edu

LIGO Hanford Observatory
Route 10, Mile Marker 2
Richland, WA 99352
Phone (509) 372-8106
Fax (509) 372-8137
E-mail: info@ligo.caltech.edu

LIGO Livingston Observatory
19100 LIGO Lane
Livingston, LA 70754
Phone (225) 686-3100
Fax (225) 686-7189
E-mail: info@ligo.caltech.edu

http://www.ligo.caltech.edu/

1 Introduction

Einstein's theory of general relativity has been successful in providing a satisfactory theoretical framework that is able to provide an explanation for several physical phenomena that Newtonian physics was incapable of doing. One of the predictions of the theory of general relativity is the gravitational wave. Measurement and characterisation of gravitational waves will be another empirical observation in support of this theory.

The physical manifestation of gravitational waves is a strain in space-time, which from a field-theory perspective can be modelled as a perturbation to the 4-dimensional Minkowski metric [1]. Measurement of this strain would then allow the characterisation of the gravitational wave. The primary difficulty in directly measuring a gravitational wave is the length-scale of the problem, set by the ratio of the universal gravitational constant, G and the fourth power of the speed of light, c [1].

$$h \sim G/c^4 \sim 8.23 \times 10^{-45} m^{-1} kg^{-1} s^2 \tag{1}$$

Thus, any attempt to measure the effects of a gravitational wave has to employ an instrument that is sensitive to extremely small strains. One such class of instruments, capable of measuring very small changes in length, are laser interferometers [2]. A schematic of how an interferometer is used to measure strain due to gravitational waves is depicted in Figure 1.

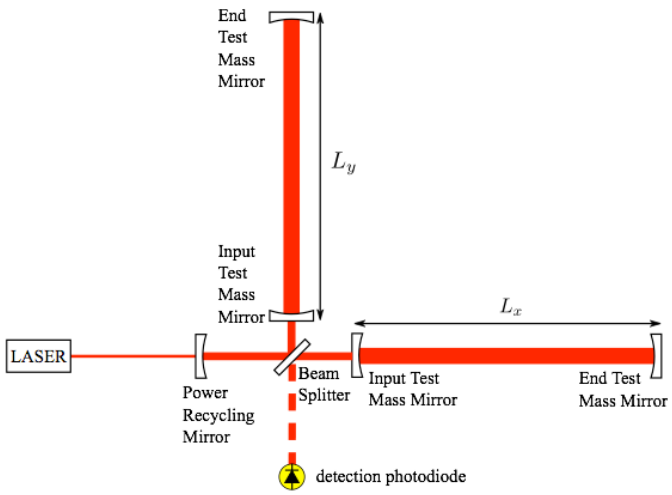

Figure 1: Diagram of a Michelson Interferometer (with Power Recycling and Fabry Perot (FP) Arm Cavities) for gravitational wave detection [3]

The end mirrors of the interferometer can be considered as free masses, which will be displaced by a passing gravitational wave. The fact that the two arms of the interferometer are orthogonal to each other means that an incident gravitational wave results in a phase difference $\Delta\phi$ (which is proportional to the differential arm length $L_x - L_y$) between the waves arriving at the Beam-Splitter from both arms.

Hence, the intensity of the recombined light is a function of the differential arm length (DARM) of the interferometer, and therefore, the intensity of the light at the detection port is proportional to the gravitational wave strain. While this scheme is simple enough in principle, there are a number of difficulties in a practical implementation of an interferometer to detect gravitational waves.

2 The Problem

There are a number of practical difficulties involved in building a gravitational wave detector. These may be broadly classified under two headings; those arising from the electronics used to track the intensities at the output ports and those arising from the interferometer parts themselves (mirrors, beam-splitters etc). I will be primarily concerned with the latter.

The difficulty is the following; if we are to indeed ascribe a change in the intensity at the output ports of the interferometer to a gravitational wave-induced strain, then it must be true that any change in the DARM must have been due to the gravitational wave alone. It is implicitly assumed that in the absence of a gravitational wave, the interferometer is perfectly still. Naturally, this assumption is not a valid one in a practical implementation of an interferometer, as there are various sources which corrupt the detector output.

Of the various degrees of freedom of the interferometer, the angular ones are particularly important. Not only do they couple to the DARM, but angular misalignment also affects the ability of the the coupled cavities of the dual power-recycled michelson interferometer to remain resonant to the main laser beam. Maintaining the angular positions of the mirrors is critical if this is to be attained. Thus, reducing unwanted angular motion is an important milestone in increasing the sensitivity of the LIGO detectors.

A number of control loops are common in interferometers. These loops sense undesirable movements of the mirrors in the interferometer (from various sources), process this information and appropriately actuate on the mirrors to counteract the movement such that the interferometer as a whole remains stationary.

3 Project Objectives and Approach

Alignment Sensing and Control (ASC) systems have been successfully commissioned before, and their performance has been evaluated in detail [3]. In designing an ASC system, the important steps are the following:

- Identify points from which the error signal is to be sensed.
- Digitize the error signal and filter it appropriately.
- Derive a feedback signal.
- Actuate using this feedback signal.

Usually, the points of actuation are the various mirrors in the cavities themselves. Implementing an ASC in this manner, however, is a formidable task as there is a fairly complex, non-linear coupling between the various cavities in the interferometer that has to be taken into account.

3.1 The Approach

The approach to be taken in this project is as follows. Two auxiliary laser beams, each located at one end-station of the interferometer (near the "End Test Mass Mirrors" in Figure 1) output beams at 1064 nm. This light is then frequency doubled to create a 532 nm beam. A control loop (explained below) will make use of the 532 nm beam to ensure that the cavity is locked to the auxiliary laser beam. The 532 nm beam serves as a sensor for measuring the angular alignment for the Fabry-Perot arm cavity. The advantage of such an approach is that we are injecting the beam through the end-mirrors of the interferometer, avoiding the coupled cavities around the beam splitter, and so get information only about our arm cavity. Thus, we avoid the aforementioned non-linear coupling between the various cavities in the interferometer.

The other pertinent point about the proposed ASC is that there is no actuation on any of the interferometer mirrors. Rather, the proposed servo actuates on a set of steering mirrors that are used to guide the auxiliary laser beam into the cavity. Any misalignment in the cavity will mean that it is no longer perfectly resonant for the 532 nm auxiliary beam. Using the intensity of transmitted light at 532 nm as a measure of whether the cavity is ideally aligned to the auxilary laser or not, we are able to actuate on the mirrors that steer the auxiliary laser into the cavity such that it remains locked to the 532 nm beam.

The power of the transmitted light from a cavity is maximum when the cavity axis and the transmission axis of the laser beam coincide perfectly. When this alignment is distrubed, the transmitted power falls. A detailed mathematical treatment of this in terms of eigenfunctions of the cavity may be found in [4] or [5], but a qualitative picture can be derived from the sketches shown in Figure 2.

The inverted parabola in the top plot in Figure 2 is representative of the transmitted power as a function of the displacement of the centre of an interferometer mirror in (say) the x-direction with $x = 0$ corresponding to the cavity being perfectly aligned. A difficulty becomes immediately apparent-because the graph is symmetric about $x = 0$, we need a means of sampling the derivative of this function in order to actuate correctly on the steering mirrors. To help solve this problem, a modulation signal is introduced in the servo loop.

The actuators used to move the steering mirrors are essentially piezoelectric transducers, composed of Lead Zirconate Titanate (henceforth referred to as PZTs). PZTs respond to an applied voltage by a change in its physical dimensions, which is the mechanism by which they actuate the steering mirrors.

The signal applied to the PZTs on the steering mirrors is a combination of the feedback signal and a small amplitude modulation signal, at frequency ω_o. A photodiode measures the transmitted power of the 532 nm beam, and a band-pass filtering stage allows us to extract the error signal at the frequency of the modulation signal.

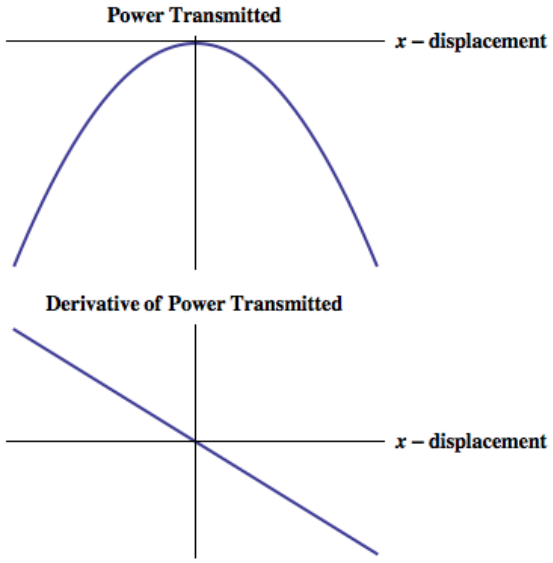

Figure 2: Transmitted Power of Auxiliary laser beam as a function of x-displacement of interferometer mirror (Top), and its derivative (Bottom)

By demodulating the error signal with the modulation signal, we get information about which side of the origin we are on.

Knowing the transfer function of the system, we can design a set of control filters, derive a feedback signal which will be fed to the PZTs. The feedback signal undergoes a low-pass filtering operation to ensure that only the first harmonic of the demodulated signal is sent to the PZTs.

A block diagram of the proposed servo, with all the elements explained above included, is shown in Figure 3.

4 Implementation

In the previous sections, I have described the conceptual framework behind this project. In this and subsequent sections, I discuss aspects pertaining to the implementation of an ASC system, the progress made thus far in this respect, and the plan of action for the coming month.

4.1 Optical Layout of the Upgraded Y-Endtable of the 40m Interferometer

The optical tables located at the end-stations of the interferometer are presently undergoing an upgrade in order to allow better stability and input pointing of the green auxiliary laser, so as to commission dither alignment. Work is proceeding independently on the X and Y arms of the interferometer.

ASC is primarily concerned with the auxiliary laser and the main elements of this system

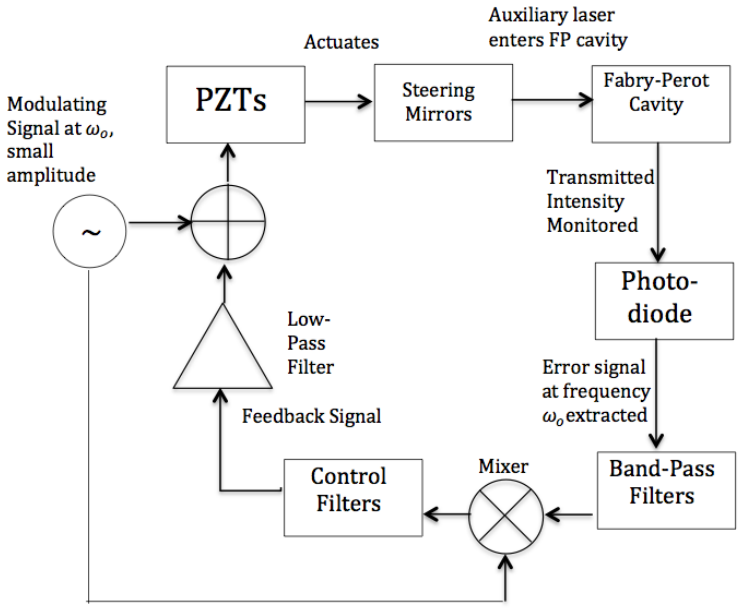

Figure 3: The Proposed Servo Design

are illustrated schematically (the actual layout of the components on the table are different) in Figure 4 for greater clarity. I have divided these components into two sections; those that deal with the polarization of the beam and the second harmonic generation, and those that are used to mode-match the auxiliary beam to the cavity.

4.1.1 The Auxiliary laser system

The first stage consists of components used to derive an appropriately polarized green beam from the auxiliary laser. The auxiliary laser is a Non-Planar Ring Oscillator (NPRO) that emits a beam at 1064 nm. The main beam in the interferometer is p-polarized and hence, all the optics in the main interferometer are chosen to work with p-polarized light. Since the auxiliary laser beam is going to encounter the end and input test masses (ETMs and ITMs) while it traverses the FP arm cavity, it is necessary to ensure that it too, is p-polarized. It is to this end that the Quarter-Wave-Plate (QWP) and Half-Wave-Plate (HWP) are placed immediately after the auxiliary laser.

The first of two Faraday isolators in this system (designed for 1064 nm light) ensures that no light is reflected back from the interferometer to the laser. The 1064 nm beam then enters a second harmonic generation (SHG) crystal which doubles the frequency of the incident light and emits a beam composed of light at 1064 nm and 532 nm. A harmonic separator is used to reject the 1064 nm content (the power in this component of the beam is dumped in a razor beam dump). The beam then enters a second Faraday isolator (designed for 532 nm light).

The second stage consists of optics used to mode-match the waist of the green beam in the

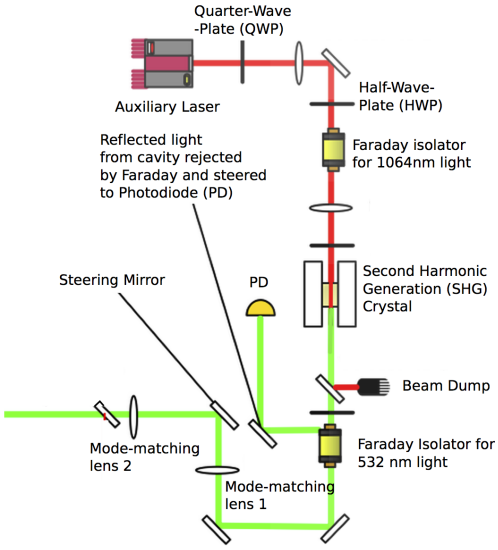

Figure 4: Main elements of the Auxiliary laser system [14].

FP arm cavity to that of the main beam. There are three steering mirrors and two lenses which allow the shaping of the beam as it propagates (discussed in greater detail in the next section). The beam then enters the FP arm cavity, while the rejcted beam from the Faraday isolator is steered using a mirror to a photodiode. This signal from this photodiode will serve as the error signal for the ASC servo to be implemented.

4.2 Mode-matching the Auxiliary laser to the FP arm cavity

Before the mirrors could be installed on their PZT mounts, the green beam had to be mode-matched to the FP arm cavity. In this section, I briefly review Gaussian beam propagation and mode-matching techniques, as well as how we attempted to find a mode-matching solution that met our requirements.

4.2.1 Gaussian beam propagation

The auxiliary laser is oscillating in the TEM_{00} mode [9] which means that it emits a beam that has a transverse intensity profile that can be modelled using Gaussian functions. If the beam is propagating along the $z-$direction, then its intensity profile in a plane transverse to the direction of propagation (i.e. the $x-y$ plane) may be modelled as

$$I(r,z) = I_o(z)e^{-2r^2/w^2(z)} \tag{2}$$

where $I_o(z)$ is the peak intensity at z, r is the transverse radial distance from the $z-$axis, and w is that radial distance at which the intensity drops to $I_o(z)e^{-2}$. Thus, practically all

the energy in the beam is contained within an imaginary cylindier of radius w[2], and when we speak of the spot-size of the beam, it is really a circle of radius w that is being referred to. The minimum value attained by w is called the beam-waist, and is denoted by w_o

The propagation of such a Gaussian beam is modelled by the following equation (setting the position of the beam-waist at $z = 0$):

$$w(z) = w_o[1 + (\frac{\lambda z}{\pi w_o^2})^2]^{1/2} \tag{3}$$

Figure 5 illustrates the propagation of a Gaussian beam as well as the location of the beam waist.

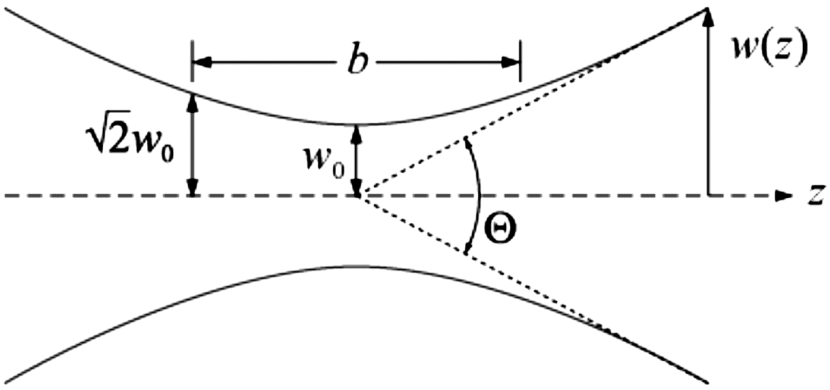

Figure 5: Propagation of a Gaussian beam. The beam waist is marked w_o

It is desirable to have control over the location of the beam waist and the spot size of the beam at various points along its path. In particular, the beam entering the FP arm cavity must be such that it is resonant within the cavity. This is done using a combination of lenses placed at specific locations on the beam path. The procedure is called mode-matching.

4.2.2 Mode-matching a laser beam to an optical cavity

The propagation of Gaussian beams through optical components such as lenses and optical cavities can be modelled using transfer matrices under the paraxial approximation [10]. These transfer matrices are commonly referred to as ABCD matrices by virtue of them being 2-by-2 matrices whose elements are characteristic of the optical component and its position. When multiple optical components are present, the ABCD matrix characterising the compound optical system can be obtained by multiplying the individual components' ABCD matrices.

Figure 6 illustrates the propagation of a beam through an optical component.

The transfer matrix relation for the situation depicted in Figure 6 is as follows;

$$\begin{bmatrix} h_2 \\ h_2' \end{bmatrix} = \begin{bmatrix} A & B \\ C & D \end{bmatrix} \begin{bmatrix} h_1 \\ h_1' \end{bmatrix} \tag{4}$$

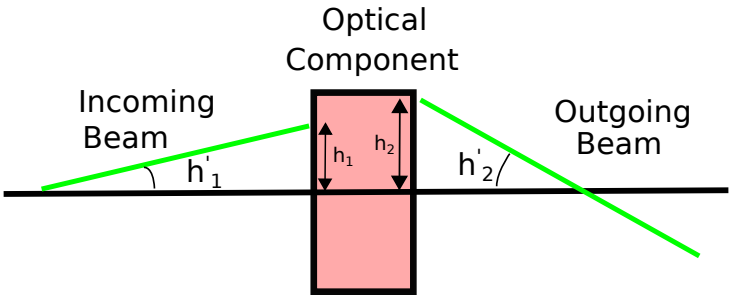

Figure 6: Propagation of a beam through an optical component

Thus, knowing the ABCD matrix for a given optical component, and the parameters characterising the incoming beam (h_1 and $h_1^{'}$), we can calculate the parameters characterising the output beam.

In attempting to mode-match the green beam from the auxiliary laser to the FP cavity, we had to find a combination of lenses that results in a beam of the desired profile entering the cavity. In reality, this is a complex optimization problem which does not have a unique solution. The problem was further complicated by the fact that there are 5 optical components in the compound system, namely three lenses, the ETM and the ITM. Of these, the positions of the ETM, ITM and one lens is fixed. The goal then was to find two lenses of suitable focal lengths and put them in the right positions such that the waist of the beam in the cavity was at the ITM, which was necessary for the auxiliary laser beam to be resonant in the TEM_{00} mode within the FP arm cavity.

We used a MATLAB package called 'a la mode' [11] to solve this optimization problem. The input parameters fed into the script were the characteristics of the input beam (i.e. the beam from the second Faraday isolator shown in Figure 4), the position and size of the desired beam-waist, positions of the fixed optical elements, and a list of available lenses to choose from.

Despite the package simplifying the computation significantly, realizing this solution physically was a challenging task due to the following reasons:

- The MATLAB package assumes thin lenses which is an idealization of the actual scenario, where the lenses have finite thickness.
- A la mode is very sensitive to the inital values fed to it, as well as the tolerances used to reject candidate lens combinations. Thus, it is difficult to systematically identify the 'best' solution as different initial conditions and tolerances tend to yield different solutions.
- The cross-section of the beam from the auxiliary laser is elliptical rather than circular, which is what the script assumes.
- The alignment of the steering mirrors was crucial in determining if the right mode-matching solution had been realised. Even with the right lenses at the right place,

an improperly aligned beam going into the interferometer would mean that the beam would resonate at some higher order mode than the desired TEM_{00}.

We adopted the following measures:

- In order to minimize the effect of the non-ideality of the lenses, we placed the first lens at the location where the spot size of the actual beam matched that in the MATLAB simulation. We then fine-tuned the position of the lens such that the beam emerging from it had the same size as the corresponding beam in the simulation. This effectively simplified the problem to accurately positioning one lens.

- Of the candidate solutions obtained, we chose the combination of lenses that was least sensitive to the position of the second lens, which was the one that had to be tuned. A la mode parametrizes sensitivity to the position of a lens using its axial displacement matrix element, A.

  The power P remaining in the TEM_{00} mode if an optical component with axial displacement matrix element A is displaced through Δz is $P = 1 - (A\Delta z)^2$. Thus, the solution chosen had the smallest sensitivity among all the candidate solutions for the second of the two mode-matching lenses (marked L2 in Figure 7).

- In order to account for an elliptical beam, the square-root of the x and y beam radii were fed into the simulation.

The eventual solution we used is shown in Figure 7. Figure 8 is zoomed so as to show the beam propagation between the origin and the ETM. The two mode-matching lenses have focal lengths of 15 cm and 25 cm. The numbers shown are from the simulation, and some tuning of the positions of the two lenses had to be done in order to realise the solution.

The actual layout on the optical table is shown on the left in Figure 9, with the mode-matching lenses marked. The path taken by the rejected beam from the Faraday isolator, which serves as the error signal for the servo that locks the auxiliary laser to the cavity, is shown in the figure on the right.

4.3 Locking the auxiliary laser to the cavity

Once the green beam was mode-matched to the FP arm cavity, the next task was to use the reflected light from the cavity to lock the beam to the cavity. The scheme used to realise this is the Pound-Drever-Hall (PDH) locking technique. The PDH technique can be used to lock a cavity to a laser, or a laser to a cavity [12], depending on the point of actuation. For length-sensing and stabilization of the FP arm cavity, we require that the auxiliary laser beam be locked to the cavity, and thus, it is the latter scheme that is followed. The general layout of the PDH feedback loop implemented is shown in Figure 10.

The crystal resonator in the auxiliary laser is mounted with a piezoelectric element. Applying a voltage to this results in a strain being set up in the crystal resonator, which in turn varies the laser frequency [9]. When the auxiliary laser beam is resonant to the FP arm cavity, the power in the light reflected from the cavity is minimum.

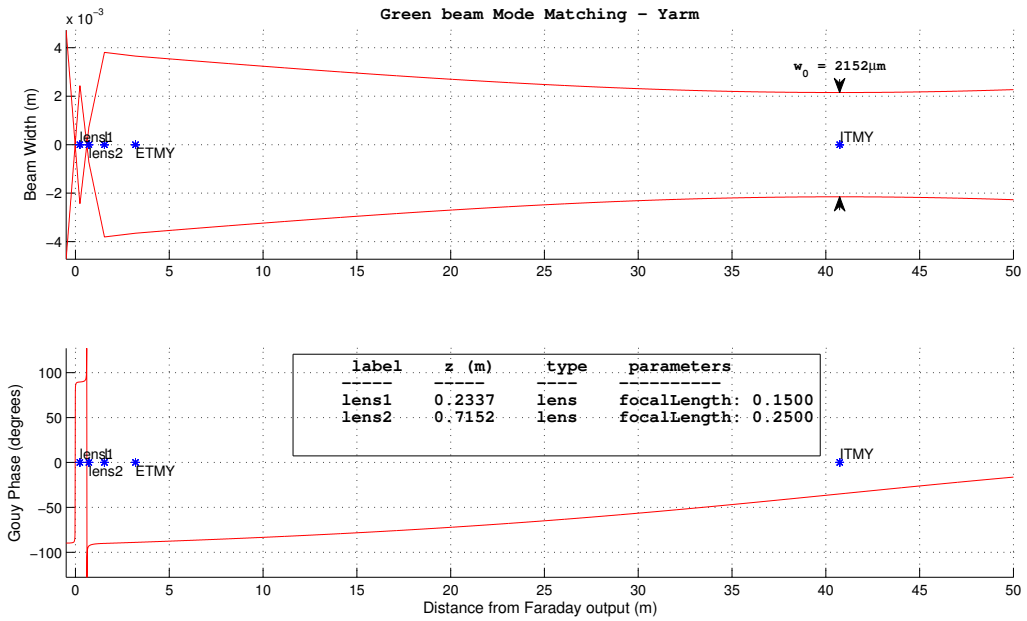

Figure 7: Mode-matching solution given by MATLAB. The origin of the coordinate system is the end of the second Faraday isolator in the beam path as shown in Figure 4 , while the target beam waist is 2.152 mm and is located at ITM Y.

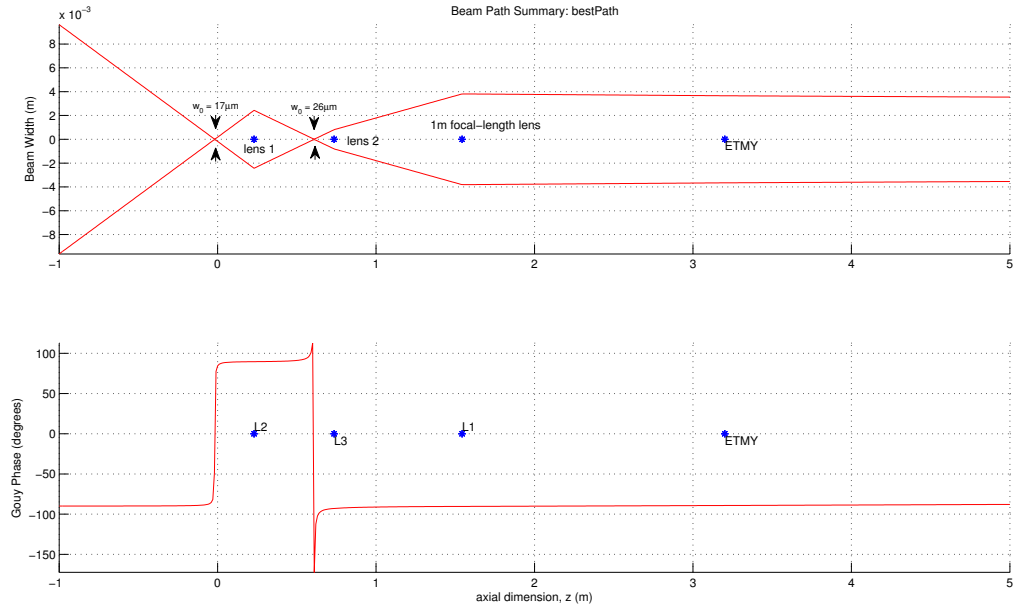

Figure 8: Beam propagation from the end of the Faraday isolator to the ETM. Mode-matching lenses are marked.

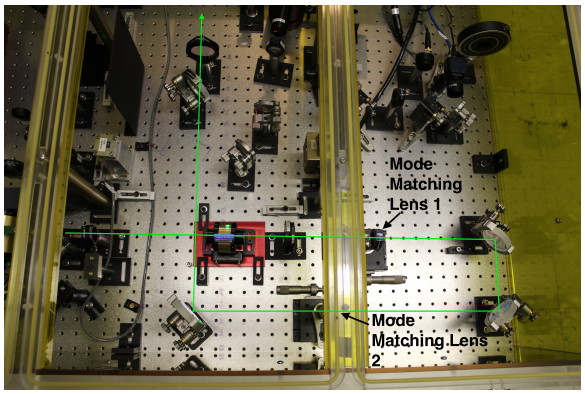

(a) Positions of the mode-matching lenses, and the path traced by the green beam before entering the FP arm cavity

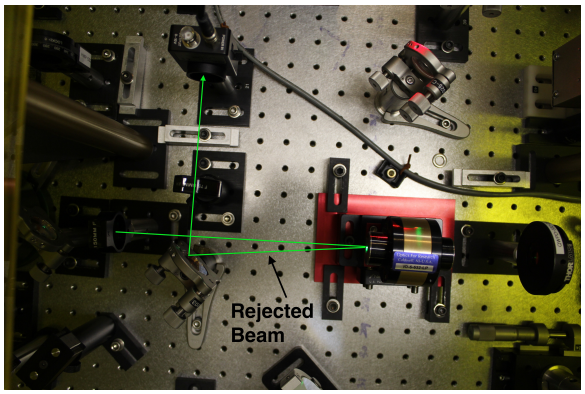

(b) Path traced by the rejected beam from the Faraday isolator

Figure 9: Physical layout of components on the endtable.

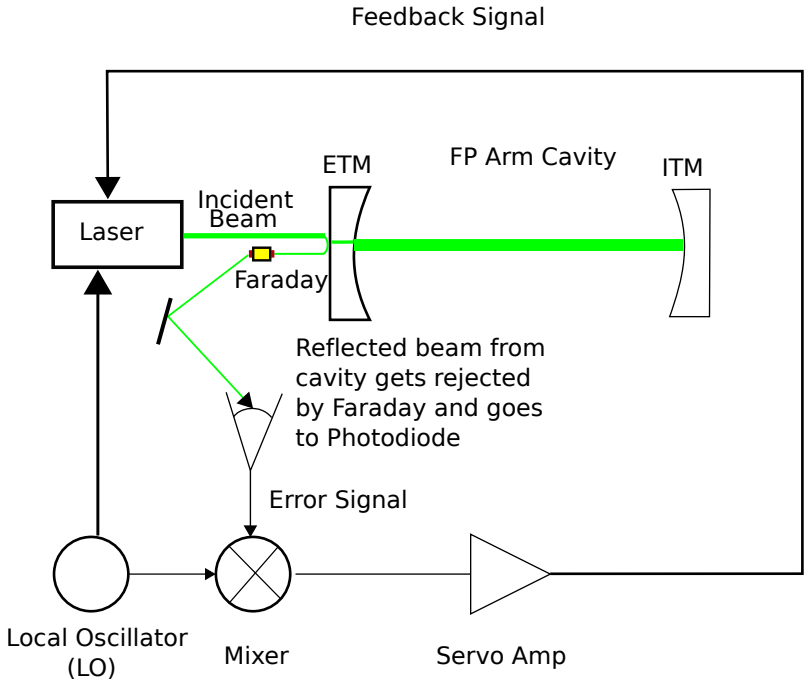

Figure 10: The general layout for locking the auxiliary laser to the FP arm cavity. Part of the incident light from the auxiliary laser is transmitted through the ETM and is resonant in the cavity, while part of it gets reflected. The reflected beam is rejected by the Faraday isolator and serves as the error signal for the loop.

LIGO has developed a Universal PDH Servo that is used for PDH locking [13], which was customised to lock the auxiliary laser to the FP arm cavity according to the scheme shown in Figure 10. It takes as inputs the error-signal and the signal from the Local Oscillator, and outputs a feedback signal.

The initial attempt to lock the auxiliary laser to the cavity was unsuccessful. The viewports used to monitor the resonant beam inside the FP arm cavity indicated that the beam was resonant in the TEM_{00} spatial mode, but the power in the beam was much lower than what was expected. Furthermore, when the PDH loop was opened, much stronger 'flashes' of the TEM_{00} mode were observed, in the brief instances when the cavity alignment happened to be such that the beam was resonant in it. The problem was eventually identified to be sideband-locking, which is described below.

A mathematical model for the scheme shown in Figure 10 is given in [12]. The pertinent point is that the modulation applied by the LO results in essentially three laser beams being incident on the cavity, one at the carrier (unmodulated) frequency ω, and two sidebands, at frequencies $\omega \pm \Omega$ where $\Omega \approx 218kHz$ is the modulation frequency of the LO.

Figure 11 is a plot of the PDH error signal. It is seen that there are three zero crossings, which occur whenever either of the three incident beams is resonant inside the cavity. The zero-crossing at the origin indicates the point at which the carrier is resonant, while the other two correspond to the sidebands being resonant.

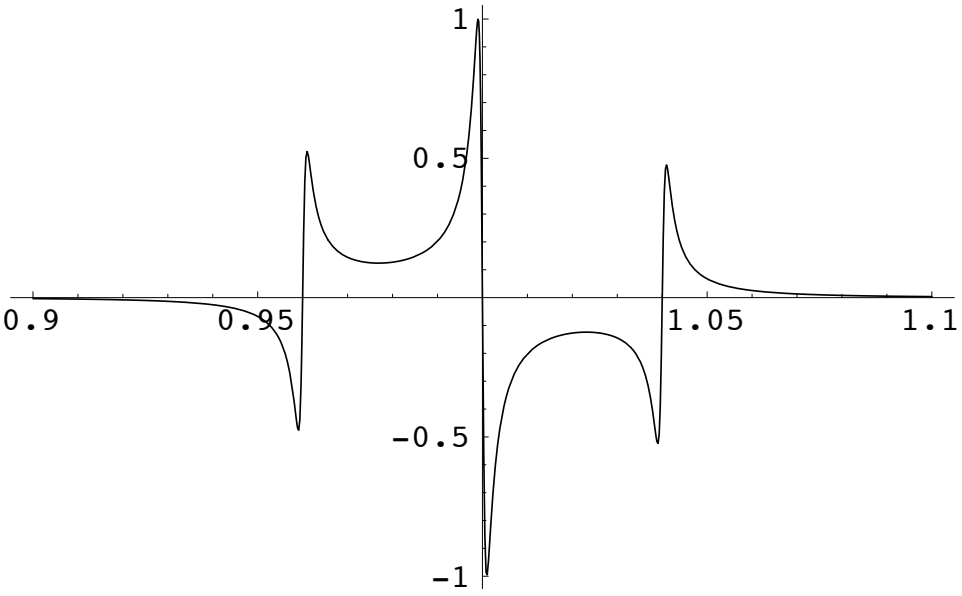

Figure 11: A plot of the PDH error signal [12]. The error signal goes to zero whenever any of the three incident beams (carrier and two sidebands) is resonant inside the cavity.

When the error signal goes to zero, the feedback loop ceases to actuate on the laser to change its frequency. As pointed out in [12], the sign of the slope of the error signal is opposite for the carrier and the sidebands. Thus, it is possible that if positive, rather than negative

feedback is applied, the cavity gets locked to one of the sidebands, which holds less power than the carrier (the ratio $\frac{Power_{carrier}}{Power_{sidebands}} = \frac{J_0^2(\beta)}{J_1^2(\beta)}$ where J_0 and J_1 are the zeroth and first order Bessel functions, β is the modulation depth). This was rectified by introducing an additional phase shift of 180^o in the feedback signal, to ensure that the feedback was truly negative. At the time of writing, the PDH servo is capable of locking the carrier beam of the auxiliary laser to the FP arm cavity in the TEM_{00} mode.

5 Plan of Action

The primary focus in the last three weeks has been to get the auxiliary green beam mode-matched to the FP arm cavity and to get the carrier beam locked to the cavity using the PDH technique. It remains to measure the transfer function of the PDH loop and also fine tune the position of the mode-matching lenses so as to achieve the best possible mode-matching of the auxiliary beam to the cavity.

Once these goals have been achieved, the PZT-mounted steering mirrors can be installed on the endtable. Some sort of calibration of the PZT-mounted mirrors will have to be done in order to get an idea of what applied voltage corresponds to what angular displacement of the mirrors. This will involve a substantial amount of planning because the following will have to be addressed;

- The PZTs require a high-voltage power supply to operate. An appropriate location will have to be identified for the high-voltage supply.
- The mirrors will first have to be glued onto the PZTs, and subsequently, mounted onto the PZT mounts. These will then have to be installed on the optical table at the end-station.
- The appropriate interfacing electronics will have to be set up in order to get the error signal into the digital domain via an analog-to-digital converter (ADC), and to get the feedback signal from the digital-to-analog converter (DAC) to the PZTs. I will need to order some SMB-to-single-lemo adaptors to this end. I will also need to come up with a diagram illustrating the various pieces of hardware (particularly the connectors) in the signal chain from the point at which the error signal is tapped, to the point of actuation. Free ADC and DAC channels which can be used will also have to be identified.

Once the hardware has been installed, the design and implementation of the software ASC servo can begin. This will be based on an existing servo called the ASS. One of the main challenges in designing and implementing this servo will be the measurement of the input and output matrices which characterize the servo.

My targets for the coming weeks are summarized in the following table.

Table 1: Proposed Project Timeline

Week No.	Task
4	Identify the required interfacing components required and order components that are presently not available in the lab. Get all the hardware ready for installation in Week 5. Perform measurement of PDH loop transfer function and fine-tune mode-matching.
5-6	Installation of hardware. Calibration of PZTs, measurement of transfer function, and implementation of first version of servo (including software integration)
7-8	Testing, troubleshooting and modifications to servo
9-10	Implementation of a second version of servo

References

[1] Peter R. Saulson *Physics of Gravitational Wave Detection: Resonant and Interferometric Detectors* Proceedings of the XXVI SLAC Summer Institute on Particle Physics: Gravity from the Hubble Length to the Planck Length (1998)

[2] Eugene Hecht, A.R. Ganesan *Optics*. Pearson, Fourth Edition (2010).

[3] Katherine Laird Dooley, *Design and Performance of High Laser Power Interferometers for Gravitational Wave Detection* (2011) PhD Thesis

[4] Dana Z. Anderson, *Alignment of Resonant Optical Cavities* (2011) Applied Optics, Vol. 23, Issue 17, pp. 2944-2949 (1984)

[5] K. Kawabe, N. Mio, K. Tsubono, *Automatic Alignment-Control System for a Suspended Fabry-Perot Cavity* Applied Optics, Vol. 33, Issue 24, pp. 5498-5505 (1994)

[6] John Bechhoefer, *Feedback for Physicists: A Tutorial Essay on Control* Reviews Of Modern Physics, Volume 77, July 2005

[7] Matt Evans, Peter Fritschel, David McClelland, John Miller, Adam Mullavey, Daniel Shaddock, Bram Slagmolen, Sam Waldman, et. al. *Advanced LIGO Arm Length Stabilisation System Design* LIGO Technical Note T0900144-v4-D, June 2010

[8] http://nodus.ligo.caltech.edu:8080/40m/8543

[9] JDSU Continuous Wave (CW) Infrared Laser-NPRO 125/126 Series Datasheet http://www.jdsu.com/ProductLiterature/npro125126-ds-cl-ae.pdf

[10] H. Kogelnik and T. Li *Laser Beams and Resonators* LIGO Publication P660001-00-R

[11] A la Mode-mode matching and beam propagation solutions for MATLAB https://github.com/nicolassmith/alm

[12] Eric Black, *LIGO Technical Note-T980045-00-D: Notes on the Pound-Drever-Hall Technique* (1998)

[13] *Universal PDH Servo* LIGO Document D0901351-v2

[14] https://wiki-40m.ligo.caltech.edu/Advanced_Techniques/Green_Locking?action=AttachFile&do=view&target=green_optics.png